

Figure 4. *In vitro* anti-angiogenic activity of tumor-derived ANGPTL4 and its molecular mechanisms. (a) Suppression of vascular tube formation by ANGPTL4. A conditioned medium was prepared by mixing the medium of subconfluent MKN28 cells expressing control or *ANGPTL4* and the HUVEC medium with VEGF-A (10 ng/ml) at 1:2. HUVECs on feeder neonatal normal human dermal fibroblast cells (Angiogenesis Kit, Kurabo, Osaka, Japan) arrived from the manufacturer on day 0, and the conditioned medium was supplemented on days 1, 4, 7 and 9. On day 11, cells were fixed and endothelial tubes were stained with anti-CD31 antibody (BD Pharmingen, San Diego, CA, USA). The experiment was conducted in triplicate. Scale bars, 50 μ m. (b) Quantification of the extent of vascular tube formation. Four parameters were scored in nine visual fields per well using the angiogenesis quantification software (Kurabo), and all the four parameters were shown to be suppressed by ANGPTL4. The results are shown as a mean \pm s.d. $*P < 0.001$ (Student's *t*-test). (c) Suppression of the HUVEC growth by ANGPTL4, but not by its mutant with the deletion. HUVECs were seeded at a density of 1×10^5 cells/10-cm dish on day 0, and the conditioned medium prepared as in a was supplemented on days 1, 3 and 5. The number of cells was counted on day 3 and day 6 by a Countess Automated Cell Counter (Invitrogen, Carlsbad, CA, USA). Each culture was carried out three times, and the result is shown as a mean \pm s.d. $*P = 8.4 \times 10^{-4}$, $**P = 5.5 \times 10^{-5}$ (Student's *t*-test). (d) The effects of ANGPTL4 and its mutant with the deletion on the cell cycle of HUVECs. The HUVECs on day 6 of c were stained with propidium iodide, and cell populations in different phases of the cell cycle were determined by a FACS Caliber flow cytometer (Becton Dickinson, San Diego, CA). S-phase arrest was observed in HUVECs exposed to ANGPTL4, but not to its mutant with the deletion. $*P < 0.05$, $**P < 0.01$ (Student's *t*-test). (e) Immunoblot analysis of various signal molecules in HUVECs on day 6 of c. Decrease of pERK1/2 and increase of pMEK1/2 were induced by ANGPTL4 and also by its mutant with the deletion. This was considered because the deletion mutation affected mainly the interaction between ANGPTL4 and extracellular matrix, which was not necessary for this analysis. Primary antibodies used include anti-phospho-ERK1/2 (1:100, Cell Signaling Technology, Danvers, MA, USA), anti-total ERK1/2 (1:100, Cell Signaling Technology), anti-phospho-MEK1/2 (1:1000, Cell Signaling Technology), anti-total MEK1/2 (1:100, Cell Signaling Technology), anti-p21 (1:200, Cell Signaling Technology), anti-cleaved Caspase-3 (Asp175) (1:200, Cell Signaling Technology), anti-cleaved PARP (Asp214) (1:200, Cell Signaling Technology) and anti-actin (1:1000, Santa Cruz Biotechnology, Santa Cruz, CA, USA). Secondary antibodies conjugated to horseradish peroxidase were obtained from Cell Signaling Technology.

Figure 3. Inhibition of tumor angiogenesis by *ANGPTL4*, but not by its mutant with the deletion. (a) Macroscopic view of the Matrigel plugs recovered in the Matrigel plug assay. Matrigel (Matrigel basement membrane matrix high concentration, phenol red-free, BD Biosciences) was mixed with the MKN28 cells (5×10^6 cells) expressing control, *ANGPTL4*, or its mutant with the deletion. The Matrigel plug was subcutaneously injected into 5-week-old female athymic nude mice on day 1, and was recovered on day 10. Marked inhibition of tumor angiogenesis by *ANGPTL4*, but not by its mutant with the deletion, was observed. Brown color shows infiltration of blood vessels into the Matrigel plugs. (b) Hemoglobin content in the Matrigel plugs ($N = 10$). The plugs were homogenized in red blood cell-lysing buffer (Sigma-Aldrich, St Louis, MO, USA), and the supernatants were measured with Drabkin's reagent (Sigma-Aldrich) to quantify the hemoglobin content in the plug. The content is shown as a mean \pm s.d. ($N = 10$). $*P = 8.0 \times 10^{-4}$, $**P = 1.2 \times 10^{-4}$ (Student's *t*-test).

demethylated the promoter and restored the *ANGPTL4* expression (Supplementary Figure S4). This showed methylation silencing of *ANGPTL4* in these cell lines.

Marked suppression of *in vivo* tumor growth by *ANGPTL4*, but not by a mutant with the deletion

The function of *ANGPTL4*, along with its mutant with the deletion, was examined by stably introducing wild-type or mutant *ANGPTL4* complementary DNA into MKN28 and AGS. The expression levels of the exogenous wild-type *ANGPTL4* and its mutant were kept in the range comparable to its physiological expression in gastric mucosae (Supplementary Figure S5a), and expression of *ANGPTL4* with the deletion mutation was confirmed by the amplification of a shorter size fragment (Supplementary Figure S5b).

Regarding *in vitro* effects, the *ANGPTL4* expression did not affect cell morphology, motility or cell growth (Supplementary Figures S6–S8). However, *in vivo*, sizes of engrafted tumors were strikingly suppressed by the wild-type *ANGPTL4*, markedly in AGS and almost completely in MKN28 (Figure 2). In contrast, when the mutant *ANGPTL4* was expressed in MKN28, it did not show any anti-tumorigenic effect. The presence of *ANGPTL4* mRNA and protein expression in the transplanted tumors was confirmed (Supplementary Figures S9 and S10). The role of *ANGPTL4* in tumor development and progression has been highly controversial, but our data clearly showed that *ANGPTL4* suppresses tumor formation, at least in gastric cancers.

Inhibition of tumor angiogenesis as a mechanism for tumor suppression

As a mechanism for tumor suppression by *ANGPTL4*, anti-angiogenic activity of tumor-derived *ANGPTL4* was examined. We performed an *in vivo* Matrigel plug angiogenesis assay to observe the vascularization that invades into a Matrigel³¹ using MKN28 cells with control (*EGFP*), *ANGPTL4*, and its mutant with the deletion. Ten days after subcutaneous transplantation, the Matrigel plugs containing the control cells showed a high degree of blood vessel recruitment, as visualized by the high content of hemoglobin (Figure 3) and by the staining of CD31-positive vascular endothelial cells (Supplementary Figure S11). In contrast, the Matrigel plugs containing the *ANGPTL4*-expressing cells showed a marked suppression of the blood vessel recruitment. However, *ANGPTL4* with the deletion mutation did not have such activity. The lack of the suppressive effect was in accordance with a report that the CCD was essential for the interaction with the extracellular matrix and for its *in vivo* suppressive activity.¹³ These results strongly indicated that the marked anti-angiogenic activity of tumor-derived *ANGPTL4* was the cause of the marked suppression of tumor growth by *ANGPTL4*.

Mechanisms for the anti-angiogenic activity of the tumor-derived *ANGPTL4*

The mechanisms of how tumor-derived, secreted *ANGPTL4* exerts its anti-angiogenic effect were analyzed. First, we conducted a vascular tube formation assay using human umbilical vein endothelial cells (HUVECs). A conditioned medium from *ANGPTL4*-expressing cells suppressed vascular tube formation of HUVECs, as visualized by staining with anti-CD31 antibody (Figure 4a), and all the parameters to assess vascular formation were markedly suppressed (Figure 4b). This result showed that a large part of the anti-angiogenic activity of tumor-derived *ANGPTL4* was mediated by the suppression of vascular tube formation in the tumor microenvironment.

The effect of the conditioned medium on the growth of HUVECs was then analyzed. The conditioned medium from cells expressing *ANGPTL4*, but not that from cells expressing its mutant with the deletion, suppressed the growth (Figure 4c). Cell cycle analysis showed that the conditioned medium from *ANGPTL4*-expressing

cells significantly increased the number of cells in the S phase, suggesting that it induced an S-phase arrest (Figure 4d). However, the amount of p21, a potential inducer of the S-phase arrest,³² was not increased (Figure 4e). No induction of apoptosis was observed by western blot analysis of apoptosis-related proteins, cleaved Caspase-3 and cleaved PARP (Figure 4e), or by terminal deoxynucleotidyl transferase dUTP nick end labeling (TUNEL) assay (Supplementary Figure S8).

Finally, the effect of tumor-derived *ANGPTL4* on the MAPK signaling was analyzed. The conditioned medium from the *ANGPTL4*-expressing cells clearly inhibited the phosphorylation of ERK1/2 (pERK1/2) (Figure 4e), and the phosphorylation of its immediate upstream mediator, pMEK, was in contrast increased. The conditioned medium from the cells expressing the mutant with the deletion showed a similar activity to that of the *ANGPTL4*-expressing cells. As CCD is not important for the delivery to target cells *in vitro* and the fibrinogen-like domain is important for inhibition of the Raf/MEK/ERK signaling,¹¹ it was considered that the deletion mutation did not affect the inhibition activity.

This study demonstrated that *ANGPTL4* is a mutated and methylation-silenced tumor suppressor whose product is secreted and inhibits angiogenesis. *ANGPTL4* mutation (loss-of-function) was identified for the first time in any type of cancers, and the anti-angiogenic activity of tumor-derived *ANGPTL4* was shown here also for the first time. These data warrant further research into utilizing *ANGPTL4* as a target of anti-angiogenesis cancer therapy.

CONFLICT OF INTEREST

The authors declare no conflict of interest.

ACKNOWLEDGEMENTS

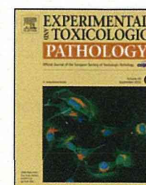
We are grateful to Dr Masabumi Shibuya, Tokyo Medical and Dental University, for his expert advice. This study was supported by the Third-term Comprehensive Cancer Control Strategy from the Ministry of Health, Labour and Welfare, Japan and by National Cancer Center Research and Development Fund. YN is a recipient of a Research Resident Fellowships from the Foundation for Promotion of Cancer Research.

REFERENCES

- Knudson AG. Two genetic hits (more or less) to cancer. *Nat Rev Cancer* 2001; **1**: 157–162.
- Baylin SB, Jones PA. A decade of exploring the cancer epigenome - biological and translational implications. *Nat Rev Cancer* 2011; **11**: 726–734.
- Kishore R, Losordo DW. Gene therapy for restenosis: biological solution to a biological problem. *J Mol Cell Cardiol* 2007; **42**: 461–468.
- Lane DP, Cheek CF, Lain S. p53-based cancer therapy. *Cold Spring Harb Perspect Biol* 2010; **2**: a001222.
- Levine AJ, Oren M. The first 30 years of p53: growing ever more complex. *Nat Rev Cancer* 2009; **9**: 749–758.
- Suzuki H, Watkins DN, Jair KW, Schuebel KE, Markowitz SD, Chen WD *et al*. Epigenetic inactivation of *SFRP* genes allows constitutive WNT signaling in colorectal cancer. *Nat Genet* 2004; **36**: 417–422.
- Shi Y, He B, You L, Jablons DM. Roles of secreted frizzled-related proteins in cancer. *Acta Pharmacol Sin* 2007; **28**: 1499–1504.
- Kaneda A, Kaminishi M, Yanagihara K, Sugimura T, Ushijima T. Identification of silencing of nine genes in human gastric cancers. *Cancer Res* 2002; **62**: 6645–6650.
- Hattori N, Okochi-Takada E, Kikuyama M, Wakabayashi M, Yamashita S, Ushijima T. Methylation silencing of angiotensin-like 4 in rat and human mammary carcinomas. *Cancer Sci* 2011; **102**: 1337–1343.
- Miida T, Hirayama S. Impacts of angiotensin-like proteins on lipoprotein metabolism and cardiovascular events. *Curr Opin Lipidol* 2010; **21**: 70–75.
- Yang YH, Wang Y, Lam KS, Yau MH, Cheng KK, Zhang J *et al*. Suppression of the Raf/MEK/ERK signaling cascade and inhibition of angiogenesis by the carboxyl terminus of angiotensin-like protein 4. *Arterioscler Thromb Vasc Biol* 2008; **28**: 835–840.

- 12 Ito Y, Oike Y, Yasunaga K, Hamada K, Miyata K, Matsumoto S *et al*. Inhibition of angiogenesis and vascular leakiness by angiotensin-related protein 4. *Cancer Res* 2003; **63**: 6651–6657.
- 13 Chomel C, Cazes A, Faye C, Bignon M, Gomez E, Ardidie-Robouant C *et al*. Interaction of the coiled-coil domain with glycosaminoglycans protects angiotensin-like 4 from proteolysis and regulates its antiangiogenic activity. *FASEB J* 2009; **23**: 940–949.
- 14 Hermann LM, Pinkerton M, Jennings K, Yang L, Grom A, Sowders D *et al*. Angiotensin-like-4 is a potential angiogenic mediator in arthritis. *Clin Immunol* 2005; **115**: 93–101.
- 15 Ma T, Jham BC, Hu J, Friedman ER, Basile JR, Molinolo A *et al*. Viral G protein-coupled receptor up-regulates Angiotensin-like 4 promoting angiogenesis and vascular permeability in Kaposi's sarcoma. *Proc Natl Acad Sci USA* 2010; **107**: 14363–14368.
- 16 Li KQ, Li WL, Peng SY, Shi XY, Tang HL, Liu YB. Anti-tumor effect of recombinant retroviral vector-mediated human ANGPTL4 gene transfection. *Chin Med J (Engl)* 2004; **117**: 1364–1369.
- 17 Galaup A, Cazes A, Le Jan S, Philippe J, Connault E, Le Coz E *et al*. Angiotensin-like 4 prevents metastasis through inhibition of vascular permeability and tumor cell motility and invasiveness. *Proc Natl Acad Sci USA* 2006; **103**: 18721–18726.
- 18 Padua D, Zhang XH, Wang Q, Nadal C, Gerald WL, Gomis RR *et al*. TGFbeta primes breast tumors for lung metastasis seeding through angiotensin-like 4. *Cell* 2008; **133**: 66–77.
- 19 Zhu P, Tan MJ, Huang RL, Tan CK, Chong HC, Pal M *et al*. Angiotensin-like 4 protein elevates the pro-survival intracellular O₂:H₂O₂ ratio and confers anoikis resistance to tumors. *Cancer Cell* 2011; **19**: 401–415.
- 20 Nakayama T, Hirakawa H, Shibata K, Abe K, Nagayasu T, Taguchi T. Expression of angiotensin-like 4 in human gastric cancer: ANGPTL4 promotes venous invasion. *Oncol Rep* 2010; **24**: 599–606.
- 21 Issa JP. CpG island methylator phenotype in cancer. *Nat Rev Cancer* 2004; **4**: 988–993.
- 22 Ushijima T. Epigenetic field for cancerization. *J Biochem Mol Biol* 2007; **40**: 142–150.
- 23 Hato T, Tabata M, Oike Y. The role of angiotensin-like proteins in angiogenesis and metabolism. *Trends Cardiovasc Med* 2008; **18**: 6–14.
- 24 Oike Y, Akao M, Kubota Y, Suda T. Angiotensin-like proteins: potential new targets for metabolic syndrome therapy. *Trends Mol Med* 2005; **11**: 473–479.
- 25 Ge H, Yang G, Huang L, Motola DL, Pourbahrami T, Li C. Oligomerization and regulated proteolytic processing of angiotensin-like protein 4. *J Biol Chem* 2004; **279**: 2038–2045.
- 26 Yin W, Romeo S, Chang S, Grishin NV, Hobbs HH, Cohen JC. Genetic variation in ANGPTL4 provides insights into protein processing and function. *J Biol Chem* 2009; **284**: 13213–13222.
- 27 Mei R, Galipeau PC, Prass C, Berno A, Ghandour G, Patil N *et al*. Genome-wide detection of allelic imbalance using human SNPs and high-density DNA arrays. *Genome Res* 2000; **10**: 1126–1137.
- 28 Hoglund M, Gorunova L, Andren-Sandberg A, Dawiskiba S, Mitelman F, Johansson B. Cytogenetic and fluorescence in situ hybridization analyses of chromosome 19 aberrations in pancreatic carcinomas: frequent loss of 19p13.3 and gain of 19q13.1–13.2. *Genes Chromosomes Cancer* 1998; **21**: 8–16.
- 29 Trojan J, Brieger A, Raedle J, Esteller M, Zeuzem S. 5'-CpG island methylation of the *LKB1/STK11* promoter and allelic loss at chromosome 19p13.3 in sporadic colorectal cancer. *Gut* 2000; **47**: 272–276.
- 30 Sobottka SB, Haase M, Fitze G, Hahn M, Schackert HK, Schackert G. Frequent loss of heterozygosity at the 19p13.3 locus without *LKB1/STK11* mutations in human carcinoma metastases to the brain. *J Neurooncol* 2000; **49**: 187–195.
- 31 Tanner JE, Forte A, Panchal C. Nucleosomes bind fibroblast growth factor-2 for increased angiogenesis *in vitro* and *in vivo*. *Mol Cancer Res* 2004; **2**: 281–288.
- 32 Zhu H, Zhang L, Wu S, Teraishi F, Davis JJ, Jacob D *et al*. Induction of S-phase arrest and p21 overexpression by a small molecule 2[[3-(2,3-dichlorophenoxy)propyl] amino]ethanol in correlation with activation of ERK. *Oncogene* 2004; **23**: 4984–4992.
- 33 Asada K, Ando T, Niwa T, Nanjo S, Watanabe N, Okochi-Takada E *et al*. *FHL1* on chromosome X is a single-hit gastrointestinal tumor-suppressor gene and contributes to the formation of an epigenetic field defect. *Oncogene* 2012; **32**: 2140–2149.
- 34 Ando T, Yoshida T, Enomoto S, Asada K, Tatematsu M, Ichinose M *et al*. DNA methylation of microRNA genes in gastric mucosae of gastric cancer patients: its possible involvement in the formation of epigenetic field defect. *Int J Cancer* 2009; **124**: 2367–2374.
- 35 Enomoto S, Maekita T, Tsukamoto T, Nakajima T, Nakazawa K, Tatematsu M *et al*. Lack of association between CpG island methylator phenotype in human gastric cancers and methylation in their background non-cancerous gastric mucosae. *Cancer Sci* 2007; **98**: 1853–1861.
- 36 Ota N, Kawakami K, Okuda T, Takehara A, Hiranuma C, Oyama K *et al*. Prognostic significance of *p16^{INK4a}* hypermethylation in non-small cell lung cancer is evident by quantitative DNA methylation analysis. *Anticancer Res* 2006; **26**: 3729–3732.

Supplementary Information accompanies this paper on the Oncogene website (<http://www.nature.com/onc>)



Napsin A is possibly useful marker to predict the tumorigenic potential of lung bronchiolo-alveolar hyperplasia in F344 rats



Masanao Yokohira^a, Sosuke Kishi^a, Keiko Yamakawa^a, Yuko Nakano^a, Fumiko Ninomiya^a, Shigemi Kinouch^b, Junko Tanizawa^b, Kousuke Saoo^a, Katsumi Imaida^{a,*}

^a Onco-Pathology, Department of Pathology and Host-Defense, Kagawa University, Kagawa 761-0793, Japan

^b Shikoku Cytopathology Laboratory, Kagawa 761-8071, Japan

ARTICLE INFO

Article history:

Received 27 June 2013

Accepted 5 November 2013

Keywords:

Napsin A

DHPN

NNK

Rat

Lung

Carcinogenesis

ABSTRACT

There are 2 types of bronchiolo-alveolar hyperplasia found in rat lungs. One is 'inflammatory hyperplasia' with a potential to recover in future with removal of the stimulating insult and the other is 'latent tumorigenic hyperplasia' as an independent preneoplastic lesion for adenocarcinoma. In the present experiment, we focused on rat lung bronchiolo-alveolar hyperplasia induced by 4-(methyl-nitrosamino)-1-(3-pyridyl)-1-butanone (NNK), which decreases with time after induction and reverts to normal, or by N-bis(2-hydroxypropyl)nitrosamine (DHPN), with tumorigenic potential to progress to adenoma and adenocarcinoma. Though NNK is a typical carcinogen inducing lung adenocarcinoma in female A/J mice, the tumorigenic potential by NNK in rats is weak. Differences between hyperplasias induced by DHPN and by NNK were here examined immunohistochemically.

Formalin fixed paraffin embedded lung samples with hyperplastic and inflammatory lesions were obtained from rats exposed to DHPN or NNK and from lung inflammation models induced with fine particles like CuO, NiO and quartz. The 19 markers were examined immunohistochemically.

Napsin A, in the inflammatory lesions and hyperplasia induced by NNK, was positive for macrophages and secretions in the alveoli spaces but less so in the walls of the alveoli. In the proliferative lesions including hyperplasia induced by DHPN, strong positive staining for napsin A was observed in the walls of the alveoli. Thus high expression was suggested to be possibly useful for detecting tumorigenic potential of rat lung hyperplasia.

© 2013 Elsevier GmbH. All rights reserved.

1. Introduction

Lung cancer is one of the most common cancers in the world, with cigarette smoking regarded as the predominant cause. The risk of lung cancer development remains elevated even after giving up smoking and second-hand environmental tobacco smoke from others is also considered to be a problem (Mitchell and Sanders, 2002). Therefore, identification of potential chemopreventive agents in animals models is important. In rodents, 4-(methyl-nitrosamino)-1-(3-pyridyl)-1-butanone (NNK) and N-bis(2-hydroxypropyl)nitrosamine (DHPN) are well known lung carcinogens, but their effects differ between rats and mice. Previously, in order to establish an appropriate bioassay for detection

of promoting potential to lung tumor after intratracheal instillation of fine particle in rats, sequential histopathological changes were examined after initiation of lung tumorigenesis by 3 intraperitoneal injections (IPs) of 10 mg NNK or 0.1% DHPN in drinking water for 2 weeks and intratracheal instillation (IT) to quartz, as a typical lung toxic agent (Yokohira et al., 2005, 2007, 2009b), into F344 male rats (Yokohira et al., 2009a). Lung proliferating lesions were seen by NNK and by DHPN in rats. However, whereas DHPN induced hyperplasias whose size, number and malignancy increased with time, NNK induced hyperplasia with inflammation proved reversible. Thus their multiplicity was 3.2 ± 2.6 (20 rats) at completion of treatment, but only 0.2 ± 0.4 (20 rats) and 0.8 ± 0.8 (20 rats) at 23 and 30 weeks, respectively. This is in line with the earlier finding that tumorigenic potential of NNK in rats is weak (Yokohira et al., 2009a). In contrast, NNK is well known as a strong lung carcinogen when administered to mice, especially to the A/J strain with high susceptibility to lung tumor induction (Takeuchi et al., 2003, 2006, 2009; Yokohira et al., 2008b). From our data there appear to be 2 types of bronchiolo-alveolar hyperplasia in the rat lungs. One is

* Corresponding author at: Onco-Pathology, Department of Pathology and Host-Defense, Faculty of Medicine, Kagawa University, 1750-1, Ikenobe, Miki-cho, Kitagun, Kagawa 761-0793, Japan. Tel.: +81 87 891 2111; fax: +81 87 891 2112.

E-mail address: imaida@med.kagawa-u.ac.jp (K. Imaida).

Table 1

Antibody for immunostaining in Experiments 1 and 2.

Antibody	Product code	Company	Antigen retrieval ^a	Dilution	Reaction time (min)
Cell proliferation					
PCNA(PC10)	sc-56	Santa Cruz Biotechnology, Inc., CA, USA	D	1:100	15
Ki67	NCL-Ki67p	Leica Microsystems Newcastle Ltd., Newcastle Upon Tyne, United Kingdom	A	1:2000	15
EGF-R	M 3563	Dako North America, Inc., CA, USA	C	1:200	15
Cell cycle					
Cyclin D1	413531	Nichirei Biosciences Inc., Tokyo, Japan	B	1:100	15
p27	M 7202	Dako Denmark A/S, Glostrup, Denmark	A	1:400	15
p53	M 7001	Dako Denmark A/S, Glostrup, Denmark	A	1:50	15
p16	CINtec p16	Roche mtm laboratories AG, Heidelberg, Germany	A	Fully diluted	15
Tumor producing					
CEA	A 115	Dako Denmark A/S, Glostrup, Denmark	D	1:100	15
Alveolar epithelium					
Napsin A	NCL-L-napsin A	Leica Microsystems Newcastle Ltd., Newcastle Upon Tyne, United Kingdom	D	1:100	15
TTF-1	M 3575	Dako North America, Inc., CA, USA	B	1:200	15
SP-A	M 4501	Dako Japan Co., Ltd., Kyoto, Japan	A	1:500	15
Cell membrane					
Cytokeratin 7	NCL-CK7-OVTL	Novocastra Laboratories Ltd., Newcastle Upon Tyne, United Kingdom	A	1:500	15
Cytokeratin 20	NCL-CK20	Leica Microsystems Newcastle Ltd., Newcastle Upon Tyne, United Kingdom	A	1:75	15
Endocrine receptor					
Estrogen receptor α	NCL-ER-6F11	Leica Microsystems Newcastle Ltd., Newcastle Upon Tyne, United Kingdom	A	1:100	15
Progesterone receptor	NCL-PGR-312	Leica Microsystems Newcastle Ltd., Newcastle Upon Tyne, United Kingdom	A	1:600	15
Chromogranin A	A 0430	Dako Denmark A/S, Glostrup, Denmark	A	1:100	15
Synaptophysin	NCL-SYNAP-299	Leica Microsystems Newcastle Ltd., Newcastle Upon Tyne, United Kingdom	A	1:100	15
Squamous cell					
Cytokeratin 34 β E12	M 0630	Dako Denmark A/S, Glostrup, Denmark	A	1:50	15
Cytokeratin 5/6	M 7237	Dako Denmark A/S, Glostrup, Denmark	A	1:50	15

^a Antigen retrieval: A: heat treatment with pH 7 reagent; B: heat treatment with pH 9 reagent; C: enzymatic treatment; D: non-treatment.

'inflammatory hyperplasia' with the potential for reversion to normal and the other is 'latent tumorigenic hyperplasia' considered as a preneoplastic precursor for adenocarcinoma.

In the present experiment, we focused on comparing rat lung hyperplasias induced by NNK and DHPN immunohistochemically. Experiments were conducted to find suitable marker(s) for prospective tumorigenic and malignant potential of early stage lung hyperplasia. To choose probable markers, preliminary staining of hyperplasias, adenomas and adenocarcinomas induced by DHPN after 30 weeks in F344 rats was performed (Experiment 1). Selected examples were then examined with hyperplasias induced by NNK or DHPN (Experiment 2). Additionally, expression of napsin A was examined in inflammatory lesions in lung induced by fine particles for comparison. Previously, lung toxicity of fine particles from various materials was examined in our *in vivo* bioassay using the IT method (Yokohira et al., 2007, 2008a, 2009b). With the same dose of 2 mg/rat IT, fine particles of quartz, CuO and NiO all caused severe toxicity with severe inflammatory changes featuring neutrophil infiltration and edema.

2. Materials and methods

2.1. Animals

Experimental animals (Experiments 1 and 2) were maintained in the Division of Animal Experiments, Life Science Research Center, Kagawa University, according to the Institutional Regulations for Animal Experiments. All of the animals were housed in polycarbonate cages with white wood chips for bedding and given free access to drinking water and a basal diet, CE-2 (CLEA Japan Inc.,

Tokyo, Japan), under controlled conditions of humidity ($60 \pm 10\%$), lighting (12-h light/dark cycle) and temperature ($24 \pm 2^\circ\text{C}$).

2.2. Experiment 1. Analysis of various markers for the lung proliferative lesions

2.2.1. Tissue samples

Formalin fixed paraffin embedded (FFPE) lung samples including neoplastic lesions (hyperplasia, adenoma and adenocarcinoma) were obtained with the rat DHPN induced lung carcinogenesis model (Yokohira et al., 2009a). Briefly, male 6-week old F344/DuCrIcrIj rats (Japan Charles River, Inc., Kanagawa, Japan) were given 0.1% DHPN (Nacalai Tesque Inc., Kyoto, Japan) in drinking water for 2 weeks, and sacrificed at week 30. At autopsy, the lungs were removed and the lungs, including the trachea and heart, were infused from the trachea with 10% phosphate buffered formalin and then rinsed in 10% phosphate buffered formalin. The lungs were immersed in 10% phosphate buffered formalin for approximately 48 h, and slices were routinely processed for embedding in paraffin for histopathological examination. The method to develop FFPE lung samples from harvested lungs was the same in Experiments 1 and 2.

2.3. Experiment 2. Validation of the selected markers from Experiment 1

2.3.1. Tissue samples

FFPE lung samples with hyperplastic lesions and inflammatory lesions were obtained with rat DHPN or NNK (Toronto Research Chemicals, ON, Canada) induced lung carcinogenesis models on week 12 and 30 (Yokohira et al., 2009a), respectively, and with

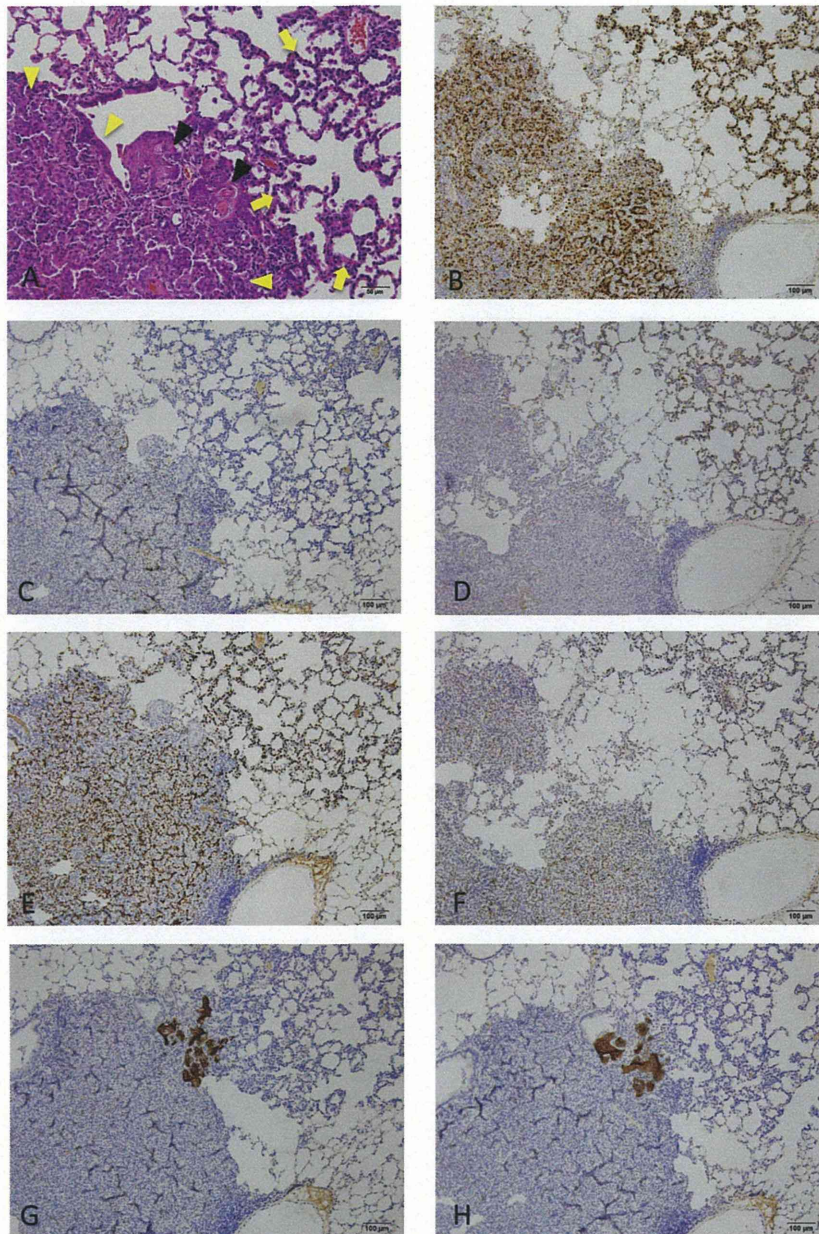


Fig. 1. Histopathological findings for the lung proliferative lesions in Experiment 1 analyzed with various markers. A, H.E.; B, cyclin D1; C, ER α ; D, napsin A; E, TTF-1; F, p27; G, cytokeratin 5/6; H, cytokeratin 34 β E12. Bar = A, 50 μ m and B–H, 100 μ m. In figure 1–A, yellow arrow-heads, black arrow-heads and yellow arrows indicate adenoma, squamous cell differentiation and hyperplasia, respectively. The markers, cyclin D1, p27, ER α , TTF-1 and napsin A, demonstrated clear staining and were selected for examination in Experiment 2. (For interpretation of the references to color in this figure legend, the reader is referred to the web version of the article.)

rat fine particle, CuO, NiO and quartz, induced lung inflammation models on day 28 (Yokohira et al., 2008a). Male 6-week old F344/DuCr1Cr1j rats were given 0.1% DHPN in drinking water for 2 weeks or 3 intraperitoneal injections of 10 mg NNNK suspended in 1 ml saline on weeks 0, 1 and 2, and sacrificed at week 12 and 30 (Yokohira et al., 2009a). Male 10-week old F344/DuCr1Cr1j rats were exposed by IT to quartz with a particle diameter less than 7 μ m (DQ-12, Deutsche Montan Technologie, DMT GmbH, Germany), CuO with a particle diameter less than 5 μ m (CAS1317-38-0, Sigma–Aldrich, MO, USA) or NiO with a particle diameter less than 10 μ m (CAS1313-99-1, Sigma–Aldrich, MO, USA) with the dose of 2 mg/rat suspended in saline (0.2 ml) (Otsuka Isotonic Sodium Chloride Solution from Otsuka Pharmaceutical Factory, Inc.,

Tokushima, Japan) on day 0, and sacrificed at day 28 (Yokohira et al., 2008a).

2.4. Histopathological analysis

Lung lesions were categorized as bronchiolo-alveolar hyperplasia and bronchiolo-alveolar adenoma in accordance with the established criteria given in 'International Harmonization of Nomenclature and Diagnostic Criteria (INHAND)' (Renne et al., 2009). In detail, bronchiolo-alveolar hyperplasia was diagnosed from the findings of solitary or multiple, segmental (cone-shaped) foci of increased cellularity, lack of strongly convex or spherical border, bronchiolo-alveolar architecture still detectable, epithelial

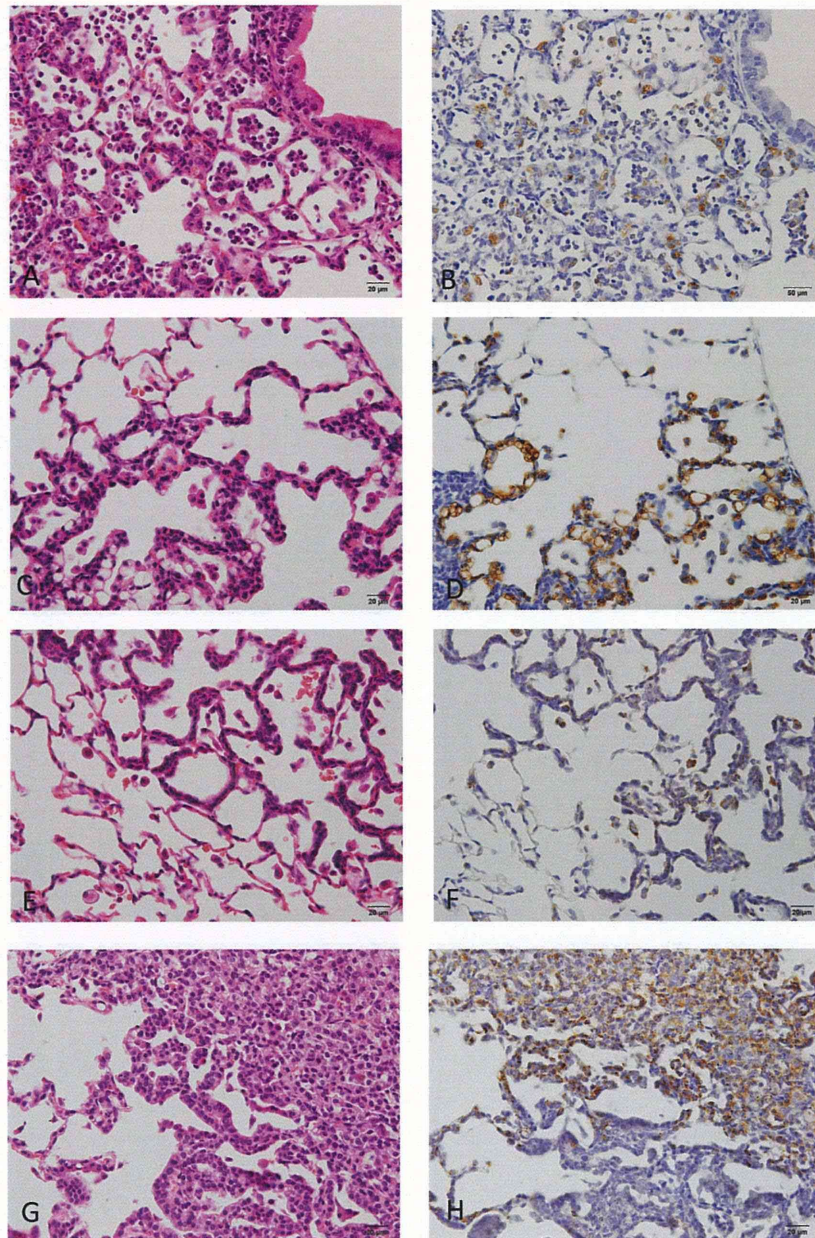


Fig. 2. Histopathological findings for napsin A in hyperplasias or adenomas in Experiment 2. A, H.E. hyperplasia and inflammation 12 weeks after treatment with NNK; B, napsin A in lung 12 weeks after treatment with NNK; C, H.E. hyperplasia after 12 weeks in lung treated with DHPN; D, napsin A after 12 weeks in lung treated with DHPN; E, H.E. hyperplasia and inflammation after 30 weeks in lung treated with NNK and quartz; F, napsin A after 30 weeks in lung treated with NNK and quartz; G, H.E. of hyperplasia and adenoma after 30 weeks in lung treated with DHPN; H, napsin A after 30 weeks in lung treated with DHPN. Bar = 20 µm. In proliferative lesions including hyperplasia, walls of the alveoli are strongly positive for napsin A. In inflammatory lesions, macrophages in the alveoli are positive for napsin A, but walls of the alveoli less so (A and B).

cells dominant and are the cause of hypercellularity, and epithelial cells usually single layered. Bronchiolo-alveolar adenoma was from frequently located at the lung periphery and usually small in size (in mice less than 3–4 mm in diameter), well-circumscribed areas of high epithelial cell density, usually with strongly convex border, underlying alveolar architecture obscured to various degrees, sharp demarcation from the surrounding tissue, neoplastic epithelial cells relatively uniform mitotic figures are rare or absent, small foci of mild atypia may be present, and occasionally extend into adjacent bronchioles.

Lungs were immunostained by the avidin–biotin complex (ABC) method, all staining processes from deparaffinization to counter-staining with hematoxylin being performed automatically using

the LEICA BOND-III™ staining system (Leica Biosystems, Nussloch, Germany). In experiment 1, marker antibodies examined were cyclin D1, napsin A, p27, thyroid transcription factor 1 (TTF-1), Ki-67, cytokeratin (CK) 7, CK 20, CK 34βE12, CK 5/6, surfactant proteins-A (SP-A), p53, endothelial growth factor receptor (EGF-R), estrogen receptor α (ERα), progesterone receptor (PR), carcinoembryonic antigen1 (CEA), p16, proliferating cell nuclear antigen (PCNA), chromogranin A and synaptophysin in the lung proliferative lesions. In experiment 2, cyclin D1, napsin A, p27, TTF-1 and ERα were chosen for investigation of expression in hyperplasia. Staining of napsin A in inflammatory lesions in lung tissues exposed to fine particles was also conducted. More details of the antibodies used in the experiments are summarized in Table 1. The

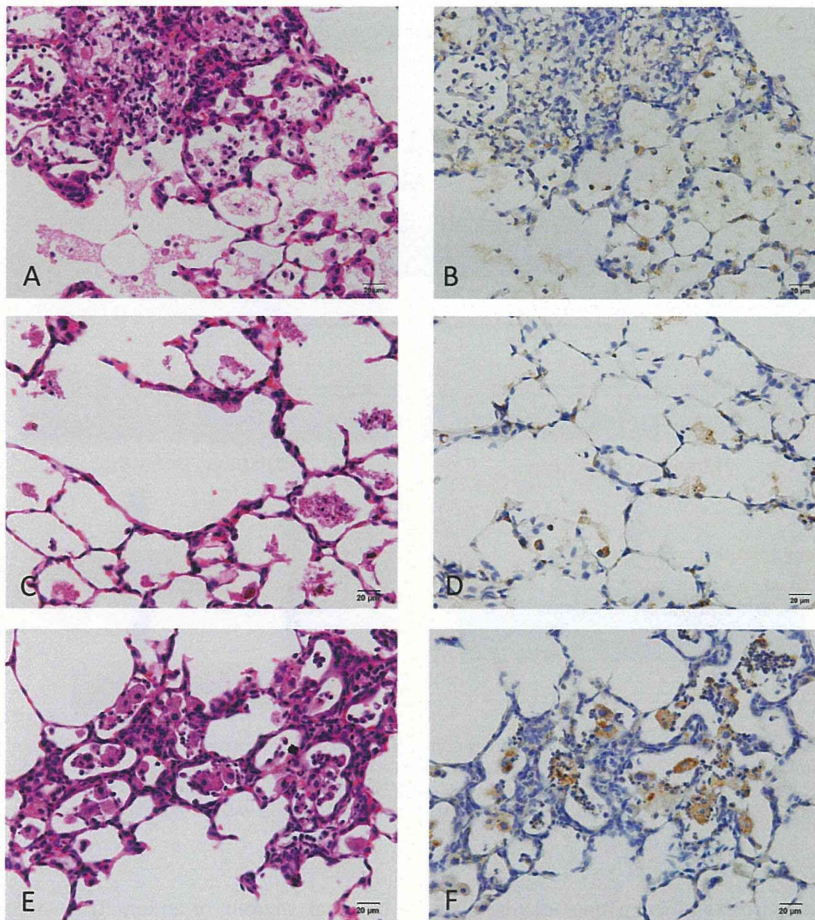


Fig. 3. Histopathological findings for napsin A in lungs with inflammation in Experiment 2. A, H.E. 28 day lung treated with quartz; B, napsin A in 28 day lung treated with quartz; C, H.E. 28 day lung treated with NiO; D, napsin A in 28 day lung treated with NiO; E, H.E. 28 day lung treated with CuO; F, napsin A in 28 day lung treated with CuO. Bar = 20 µm.

antigen retrieval was employed 3 kinds of method, heat treatment in the pressure cooker (110 °C, 5 min), enzymatic treatment (37 °C, 10 min), and non-treatment. The reagents for the heat treatment were used pH 7 buffer, instant antigen retrieval reagent (Mitsubishi Chemical Medience Co. Ltd., Tokyo, Japan), or pH9 buffer, Novocastra Bond Epitope Retrieval Solution 2 (Leica Biosystems, Tokyo, Japan). Novocastra Bond Enzyme Pretreatment Kit (Leica Biosystems, Tokyo, Japan) was for the enzymatic treatment. The reaction time for the every primary antibody was the same 15 min.

3. Results

Hyperplasias and adenomas partially with squamous cell differentiation (Fig. 1A) were noted in Experiment 1. The 10 markers of cytokeratin 7, cytokeratin 20, p53, p16, synaptophysin, chromogranin A, SP-A, PR, CEA and EGF-R, did not show any positive areas in neoplastic lesions of the lung. Strong positive staining for PCNA and Ki-67 was observed, but without differences between non-neoplastic and neoplastic lesions in the lung. Cytokeratin 5/6 and cytokeratin 34βE12 were positive for lesions with squamous cell differentiation (Fig. 1G and H). The markers, cyclin D1, ERα, napsin A, TTF-1 and p27, showed satisfactory staining (Fig. 1B, C, D, E and F, respectively) and there were seemed to be the difference between non-neoplastic lesion and neoplastic lesions to a greater or lesser degree. Therefore, the 5 markers cyclin D1, p27, ERα, TTF-1 and napsin A, were selected for examination in Experiment 2.

In Experiment 2, the selected 5 markers from the results of Experiment 1 were validated and examined in detail with the lungs with hyperplasia or adenoma. Lung lesions on 12 and 30 weeks were induced by DHPN or NNK. They were hyperplasia with inflammation in the lungs treated with NNK after 12 weeks, hyperplasia in the lung treated DHPN after 12 weeks, hyperplasia with inflammation in the lung treated with NNK after 30 weeks, and hyperplasia and adenoma in the lung treated with DHPN after 30 weeks (Fig. 2A, C, E and G). Cyclin D1 was positive for inflammation, hyperplasia and adenomas to approximately the same degree, p27 was positive for inflammation, hyperplasia and adenoma and the expression in adenoma is slightly stronger than in hyperplasia. ERα was weakly positive for inflammation, hyperplasia and adenomas but expression increased with malignant potential in tumors, evidenced by severe structural and nuclear atypia. Expression of TTF-1 was observed in hyperplasia and adenoma, especially in the walls of alveoli, to a greater extent than in inflammation. Napsin A in inflammatory lesions and hyperplasia induced by NNK was positive for macrophages and secretions in the spaces of the alveoli but less so in the actual walls. In contrast, the proliferative lesions including hyperplasia induced by DHPN demonstrated strong positive staining for napsin A in the type II cells (Fig. 2D and H), this decreasing with higher malignant potential. The markers with differences between hyperplasias induced by DHPN or NNK were TTF-1 and napsin A. The expression of napsin A in the walls of alveoli was stronger than TTF-1.

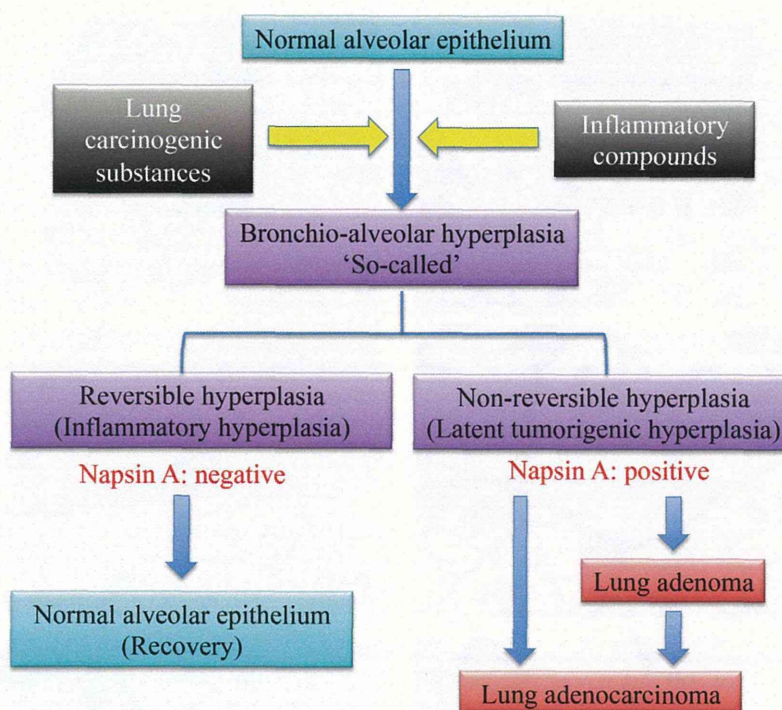


Fig. 4. Summary of features for discrimination for hyperplasia. Wall thickening of alveoli due to inflammation is not a result of proliferation of type 2 alveolar cells but rather a reaction of inflammatory cells or fibrosis. This lesion can be called “Reversible hyperplasia (inflammatory hyperplasia)”. Bronchio-alveolar hyperplasia is characterized mainly by focal increase of type 2 cells lining the inter-alveolar septa, this being termed “Nonreversible hyperplasia (latent tumorigenic hyperplasia)”. The strongly positive staining for napsin A in the walls of the alveoli in such hyperplastic lesions suggests tumorigenic potential with the possibility to progress to adenoma and adenocarcinoma in future.

Expression of napsin A was also examined in lung inflammatory lesions induced by IT of quartz, NiO or CuO at day 28 in Experiment 2 (Fig. 3). Walls of the alveoli were almost negative as in the case of NNK-induced hyperplasia (Fig. 3B, D and F).

4. Discussion

In Experiment 1, the examined markers were cyclin D1, napsin A, p27, TTF-1, Ki-67, CK 7, CK 20, CK 34 β E12, CK 5/6, SP-A, p53, EGF-R, ER α , PR, CEA, p16, PCNA, chromogranin A and synaptophysin, chosen as reflecting cell proliferation (PCNA, Ki67 and EGF-R), cell cycling (cyclin D1, p27, p53 and p16), lung alveolar cell markers (napsin A, TTF-1 and SP-A), cell membrane proteins (CK7 and CK20) to examine possibility for the modification of its expression pattern in the proliferative lesions, endocrine receptors (ER α and PR), neuroendocrine (chromogranin A and synaptophysin), squamous cell markers (CK 34 β E12 and CK 5/6) and tumor characteristics (CEA). Cyclin D1, p27, ER α , TTF-1 and napsin A showed good staining with differences, to varying degrees, in staining properties between non-proliferative and proliferative lesions and were therefore examined for potential to distinguish hyperplasia possessing tumorigenic potential.

In Experiment 2, napsin A was determined to be the best marker for detection hyperplastic lesions linked to actual neoplasia. Napsin A is an aspartic proteinase involved in the maturation of surfactant B (Beljan Perak et al., 2012), expressed in the cytoplasm of type 2 pneumocytes and Clara cells in the lung, and also in proximal tubular renal epithelium and exocrine pancreas (Bishop et al., 2010; Stoll et al., 2010). From human clinical studies, napsin A was reported to be highly specific marker for adenocarcinoma in the lung (Kadivar and Boozari, 2012; Masai et al., 2012). However, when there is a need to rule out lung metastasis from other organs, for example

by renal, thyroid, or endometrial carcinomas, implementation of other biologically specific markers should be considered (Kadivar and Boozari, 2012).

Criteria for definition and discrimination of lung hyperplasia from the results of the present experiments are summarized in Fig. 4. Hyperplasia is defined as an increase in the number of cells in an organ or tissue, usually resulting in increased volume of the organ or tissue (Kumar and Abbas, 2004). It could be physiologic which is usually reversible, or pathologic which varies in presentation from incidental to tumor-like lesions (Al-Gahtany et al., 2003). The wall thickening of alveoli with inflammation is not resultant from proliferation of type 2 alveolar cells but rather from reaction of inflammatory cells or fibrosis and thus can be called ‘reversible hyperplasia (inflammatory hyperplasia)’. This reversible hyperplasia is reported to be observed in the rat lungs after IT of zinc oxide (ZnO) (Xu et al., 2013). From the results in this experiment, immunohistochemical analysis of napsin A could identify the proliferation of lung alveolar cells. In the lung, hyperplasia is characterized mainly by focal increase of type 2 cells lining the inter-alveolar septa (Gary et al., 1990). This hyperplasia with the proliferation of the type 2 cells might be termed ‘non-reversible hyperplasia (latent tumorigenic hyperplasia)’. The strong positivity for napsin A in walls of alveoli could therefore indicate to subsequently progress to adenoma and adenocarcinoma.

Though, the markers of cyclin D1, p27, ER α and TTF-1 demonstrated strong staining in Experiment 1, they did not appear suitable for discrimination of hyperplasia types in Experiment 2. Altered expression of cyclin D1 is an early event in non-small cell lung carcinoma development, and cyclin D1 is known to be required for cells to advance from G₁ to S-phase of the cell cycle (Shishodia and Aggarwal, 2004; Weinstein, 2000). The cyclin-dependent kinase inhibitor p27 is an integral negative regulator of the cell cycle

and functions by preventing S-phase entry (Borriello et al., 2011; Hsieh et al., 2012). Expression levels of p27 protein have been reported as a significant prognostic factor in malignancies and p27-deficient mice proved susceptible to MNU induction of hyperplasia in the lung (Ogawa et al., 2011). However, in the present experiment, cyclin D1 and p27 could not distinguish inflammatory and proliferative hyperplasia. ER α exerts an augmenting effect on cell proliferation (Shimizu et al., 2012) and since it is known to be expressed in both normal lung epithelial cells and lung cancers, a possible role of estrogen has been proposed in lung carcinogenesis (Shimizu et al., 2012; Stabile et al., 2002). In the present experiment, the expression of ER α tended to be increased with higher malignant potential in lung tumors, but could not distinguish hyperplasia types. While TTF-1 is a nuclear tissue-specific DNA-binding protein mainly expressed in thyroid follicular cells, type 2 pneumocytes and non-ciliated bronchiolar epithelial cells, functioning in transcriptional activation of surfactant proteins and secretory proteins of Clara cells (Barletta et al., 2009), its expression in hyperplasia was slightly weaker than that of napsin A.

We focused on comparing rat lung bronchiolo-alveolar hyperplasias induced by NNK and DHPN, which were 'inflammatory hyperplasia' with the potential for reversion to normal and 'latent tumorigenic hyperplasia' considered as a preneoplastic precursor for adenocarcinoma, respectively. Napsin A, in the inflammatory lesions and hyperplasia induced by NNK, was positive for macrophages and secretions in the alveoli spaces but less so in the walls of the alveoli. In the proliferative lesions including hyperplasia induced by DHPN, strong positive staining for napsin A was observed in the walls of the alveoli. Therefore, napsin A was concluded to be the better marker, possibly useful as a pointer to tumorigenic potential of rat lung hyperplasias.

Conflict of interest

We have no conflicts of interest to be declared.

Acknowledgments

This work was supported in part by Grants-in-Aid for chemical risk research from the Ministry of Health, Labor and Welfare Ministry (MHLW) of Japan. We thank Dr. Malcolm A. Moore for help in critical reading of this manuscript.

References

- Al-Gahtany M, Horvath E, Kovacs K. Pituitary hyperplasia. *Hormones* 2003;2:149–58.
- Barletta JA, Perner S, Iafate AJ, Yeap BY, Weir BA, Johnson LA, et al. Clinical significance of TTF-1 protein expression and TTF-1 gene amplification in lung adenocarcinoma. *Journal of Cellular and Molecular Medicine* 2009;13:1977–86.
- Beljan Perak R, Durdov MG, Capkun V, Ivcevic V, Pavlovic A, Soljic V, et al. IMP3 can predict aggressive behaviour of lung adenocarcinoma. *Diagnostic Pathology* 2012;7:165.
- Bishop JA, Sharma R, Illei PB. Napsin A and thyroid transcription factor-1 expression in carcinomas of the lung, breast, pancreas, colon, kidney, thyroid, and malignant mesothelioma. *Human Pathology* 2010;41:20–5.
- Borriello A, Bencivenga D, Crisculo M, Caldarelli I, Cucciolla V, Tramontano A, et al. Targeting p27Kip1 protein: its relevance in the therapy of human cancer. *Expert Opinion on Therapeutic Targets* 2011;15:677–93.
- Gary AB, Scot LE, Michel RE, Charles AM, William FM. *Pathology of the Fischer Rat*. Reference and Atlas. San Diego, California: Academic Press; 1990. p. 350–7.
- Hsieh HY, Shieh JJ, Chen CJ, Pan MY, Yang SY, Lin SC, et al. Prodigiosin down-regulates SKP2 to induce p27(KIP1) stabilization and antiproliferation in human lung adenocarcinoma cells. *British Journal of Pharmacology* 2012;166:2095–108.
- Kadivar M, Boozari B. Applications and limitations of immunohistochemical expression of napsin-A in distinguishing lung adenocarcinoma from adenocarcinomas of other organs. *Applied Immunohistochemistry & Molecular Morphology: AIMM/Official Publication of the Society for Applied Immunohistochemistry* 2012;21:191–5.
- Kumar V, Abbas A. Robbins and Cotran Pathologic Basis of Disease. New York: Saunders; 2004. p. 6–7.
- Masai K, Tsuta K, Kawago M, Tatsumori T, Kinno T, Taniyama T, et al. Expression of squamous cell carcinoma markers and adenocarcinoma markers in primary pulmonary neuroendocrine carcinomas. *Applied Immunohistochemistry & Molecular Morphology: AIMM/Official Publication of the Society for Applied Immunohistochemistry* 2012;21:292–7.
- Mitchell E, Sanders J. Tobacco control in NSW: evidence supporting improved strategies to reduce exposure to environmental tobacco smoke. *New South Wales Public Health Bulletin* 2002;13:215–7.
- Ogawa K, Murasaki T, Sugiura S, Nakanishi M, Shirai T. Organ differences in the impact of p27(kip1) deficiency on carcinogenesis induced by N-methyl-N-nitrosourea. *Journal of Applied Toxicology* 2011;33:471–9.
- Renne R, Brix A, Harkema J, Herbert R, Kittel B, Lewis D, et al. Proliferative and non-proliferative lesions of the rat and mouse respiratory tract. *Toxicologic Pathology* 2009;37:55–73.
- Shimizu K, Hirami Y, Saisho S, Yukawa T, Maeda A, Yasuda K, et al. Membrane-bound estrogen receptor-alpha expression and epidermal growth factor receptor mutation are associated with a poor prognosis in lung adenocarcinoma patients. *World Journal of Surgical Oncology* 2012;10:141.
- Shishodia S, Aggarwal BB. Cyclooxygenase (COX)-2 inhibitor celecoxib abrogates activation of cigarette smoke-induced nuclear factor (NF)-kappaB by suppressing activation of IkkappaB kinase in human non-small cell lung carcinoma: correlation with suppression of cyclin D1, COX-2, and matrix metalloproteinase-9. *Cancer Research* 2004;64:5004–12.
- Stabile LP, Davis AL, Gubish CT, Hopkins TM, Luketich JD, Christie N, et al. Human non-small cell lung tumors and cells derived from normal lung express both estrogen receptor alpha and beta and show biological responses to estrogen. *Cancer Research* 2002;62:2141–50.
- Stoll LM, Johnson MW, Gabrielson E, Askin F, Clark DP, Li QK. The utility of napsin-A in the identification of primary and metastatic lung adenocarcinoma among cytologically poorly differentiated carcinomas. *Cancer Cytopathology* 2010;118:441–9.
- Takeuchi H, Saoo K, Matsuda Y, Yokohira M, Yamakawa K, Zeng Y, et al. 8-Methoxypsoralen, a potent human CYP2A6 inhibitor, inhibits lung adenocarcinoma development induced by 4-(methylnitrosamino)-1-(3-pyridyl)-1-butanone in female A/J mice. *Molecular Medicine Reports* 2009;2:585–8.
- Takeuchi H, Saoo K, Matsuda Y, Yokohira M, Yamakawa K, Zeng Y, et al. Dose dependent inhibitory effects of dietary 8-methoxypsoralen on NNK-induced lung tumorigenesis in female A/J mice. *Cancer Letters* 2006;234:232–8.
- Takeuchi H, Saoo K, Yokohira M, Ikeda M, Maeta H, Miyazaki M, et al. Pretreatment with 8-methoxypsoralen, a potent human CYP2A6 inhibitor, strongly inhibits lung tumorigenesis induced by 4-(methylnitrosamino)-1-(3-pyridyl)-1-butanone in female A/J mice. *Cancer Research* 2003;63:7581–3.
- Weinstein IB. Disorders in cell circuitry during multistage carcinogenesis: the role of homeostasis. *Carcinogenesis* 2000;21:857–64.
- Xu J, Futakuchi M, Alexander DB, Fukamachi K, Numano T, Suzui M, et al. Nano-sized zinc oxide particles do not promote DHPN-induced lung carcinogenesis but cause reversible epithelial hyperplasia of terminal bronchioles. *Archives of Toxicology* 2013 (in press).
- Yokohira M, Hashimoto N, Yamakawa K, Suzuki S, Saoo K, Kuno T, et al. Lung carcinogenic bioassay of CuO and TiO₂ nanoparticles with intratracheal instillation using F344 male rats. *Journal of Toxicologic Pathology* 2009a;22:71–8.
- Yokohira M, Kuno T, Yamakawa K, Hashimoto N, Ninomiya F, Suzuki S, et al. An intratracheal instillation bioassay system for detection of lung toxicity due to fine particles in F344 rats. *Journal of Toxicologic Pathology* 2009b;22:1–10.
- Yokohira M, Kuno T, Yamakawa K, Hosokawa K, Matsuda Y, Hashimoto N, et al. Lung toxicity of 16 fine particles on intratracheal instillation in a bioassay model using F344 male rats. *Toxicologic Pathology* 2008a;36:620–31.
- Yokohira M, Takeuchi H, Saoo K, Matsuda Y, Yamakawa K, Hosokawa K, et al. Establishment of a bioassay model for lung cancer chemoprevention initiated with 4-(methylnitrosamino)-1-(3-pyridyl)-1-butanone (NNK) in female A/J mice. *Experimental and Toxicologic Pathology: Official Journal of the Gesellschaft für Toxikologische Pathologie* 2008b;60:469–73.
- Yokohira M, Takeuchi H, Yamakawa K, Saoo K, Ikeda M, Matsuda Y, et al. Establishment of a bioassay system for detection of lung toxicity due to fine particle instillation: Sequential histopathological changes with acute and subacute lung damage due to intratracheal instillation of quartz in F344 male rats. *Journal of Toxicologic Pathology* 2005;18:13–8.
- Yokohira M, Takeuchi H, Yamakawa K, Saoo K, Matsuda Y, Zeng Y, et al. Bioassay by intratracheal instillation for detection of lung toxicity due to fine particles in F344 male rats. *Experimental and Toxicologic Pathology: Official Journal of the Gesellschaft für Toxikologische Pathologie* 2007;58:211–21.

III. 研究班員名簿

平成 23-25 年度厚生労働科学研究費補助金 化学物質リスク研究事業
 化学物質の安全性と発がん性リスク評価のための短・中期バイオアッセイ系の開発
 研究班員名簿

区分	名前	所属	職名
研究代表者	吉見 直己	琉球大学大学院医学研究科腫瘍病理学	教授
研究分担者	高橋 智	名古屋市立大学大学院医学研究科実験病態病理学	教授
	塚本 徹哉	藤田保健衛生大学医学部病理診断科	准教授
	久野 壽也	名古屋市立大学大学院医学研究科実験病態病理学	准教授
	魏 民	大阪市立大学大学院医学研究科都市環境病理学 (現. 大阪市立大学大学院医学研究科分子病理学)	准教授
	横平 政直	香川大学医学部腫瘍病理学	助教
	小川 久美子	国立医薬品食品衛生研究所安全性生物試験研究センター 病理部実験病理学	部長
	戸塚 ゆ加里	国立がん研究センター研究所発がんシステム研究分野	ユニット長
	伊吹 裕子	静岡県立大学環境科学研究所環境毒性学	准教授
協力者	西川 秋佳	国立衛試安全性生物試験研究センター	センター長
	酒々井 真澄	名古屋市立大学大学院医学研究科分子毒性学	教授
	田中 卓二	岐阜大学	非常勤講師

